

# Spatially resolved electronic structure inside and outside the vortex core of a high temperature superconductor

V. F. Mitrović\*, E. E. Sigmund\*, M. Eschrig†, H. N. Bachman\*, W. P. Halperin\*, A. P. Reyes‡, P. Kuhns‡ & W. G. Moulton‡

\* Department of Physics and Astronomy, Northwestern University, Evanston, Illinois 60208, USA

† Materials Science Division, Argonne National Laboratory, Argonne, Illinois 60439, USA

‡ National High Magnetic Field Laboratory Tallahassee, Florida 32310, USA

One of the puzzling aspects of high temperature superconductors is the prevalence of magnetism in the normal state and the persistence of superconductivity in very high magnetic fields. Generally, superconductivity and magnetism are not compatible. But recent neutron scattering results [1] indicate that antiferromagnetism can appear deep in the superconducting state in an applied magnetic field. Magnetic fields penetrate a superconductor in the form of quantized flux lines each one representing a vortex of supercurrents. Superconductivity is suppressed in the core of the vortex and it has been suggested that antiferromagnetism might develop there [2]. To address this question it is important to perform electronic structural studies with spatial resolution. Here we report on implementation of a high field NMR imaging experiment [3–5] that allows spatial resolution of the electronic behavior both inside and outside the vortex cores. Outside we find strong antiferromagnetic fluctuations, and localized inside there are electronic states rather different from those found in conventional superconductors.

Supercurrents that form a vortex are expected to decay inversely with distance from the vortex core giving rise to a spatial distribution of internal magnetic fields,  $P(H_{int})$ , shown in Fig. 1. The color coding identifies spatial positions in the lattice of vortices with their corresponding location in the field distribution for a vortex lattice. This field distribution will be the same as the NMR spectrum for any nucleus with small intrinsic broadening as is the case for  $^{17}\text{O}$  in YBCO. Its narrow spectrum in the normal state (blue trace) is shown in the figure for two of the four quadrupolar satellite resonances and compared with the vortex broadened spectrum (red trace) in the superconducting state [6,7]. We isolate the  $-1/2 \leftrightarrow -3/2$  transition giving the black trace, corresponding to the expected field distribution shown in the inset. Consequently, our NMR experiment allows a spatially resolved study of the vortex structure. During the

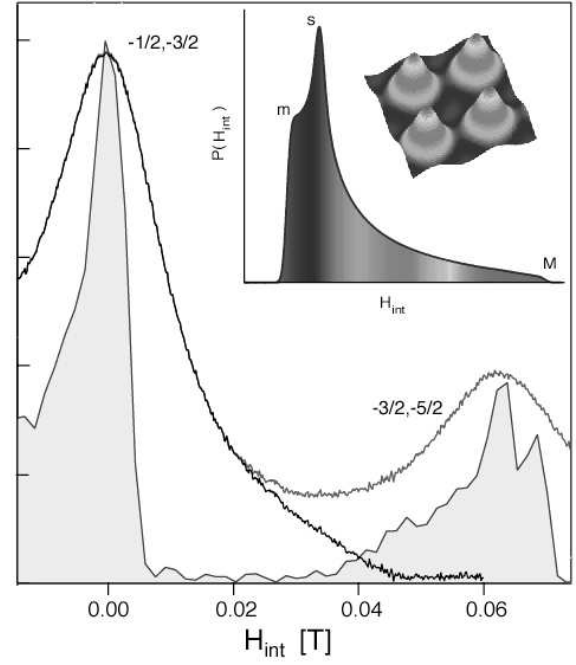


FIG. 1. Planar  $^{17}\text{O}$  spectra versus the internal magnetic field,  $H_{int}$ , showing broadening from vortices.  $H_{int} = \omega/^{17}\gamma - H_0$  where  $^{17}\gamma$  is the gyromagnetic ratio for oxygen and the spectrometer frequency,  $\omega$ , is set to resonance at the peak frequency for the  $-1/2 \leftrightarrow -3/2$  transition in the applied field  $H_0=13$  T at 11 K. For clarity only two quadrupolar satellite resonances are shown. In the normal state at 100 K (blue) there is a sharp edge which broadens at low temperature (red). The spectra are shifted such that internal fields are measured relative to the peak. The black trace represents the  $-1/2 \leftrightarrow -3/2$  part of the spectrum obtained by subtraction of the  $-3/2 \leftrightarrow -5/2$  transition. The latter was obtained from the convolution of the normal state spectrum with a broadening function measured independently on the  $3/2 \leftrightarrow 1/2$  transition (not shown here). Inset: We have calculated [8] the internal magnetic field profile and the corresponding field distribution function for a  $80^\circ$  vortex lattice at  $H_0=13$  T, with a penetration depth of  $\lambda = 1500$  Å. The minimum field at the center of the vortex lattice unit cell (m), the maximum field at the vortex cores (M), and the saddle-point field midway between vortices (s), are shown.

NMR experiment the oxygen nuclei are perturbed and then relax back to thermal equilibrium at the spin-lattice relaxation rate, which is determined by the density of electronic states near the Fermi energy. We have made spin-lattice relaxation rate measurements, Fig. 2, that are also spatially resolved and we interpret our results in terms of the electronic excitation spectrum both inside and outside the vortex cores. Within the core we expect NMR to be sensitive to localized electronic states such as have been observed in conventional superconductors [9] and recently in high temperature superconductors

[13,14]. High magnetic fields allow us to use the Zeeman effect to study such electronic excitations. Varying the

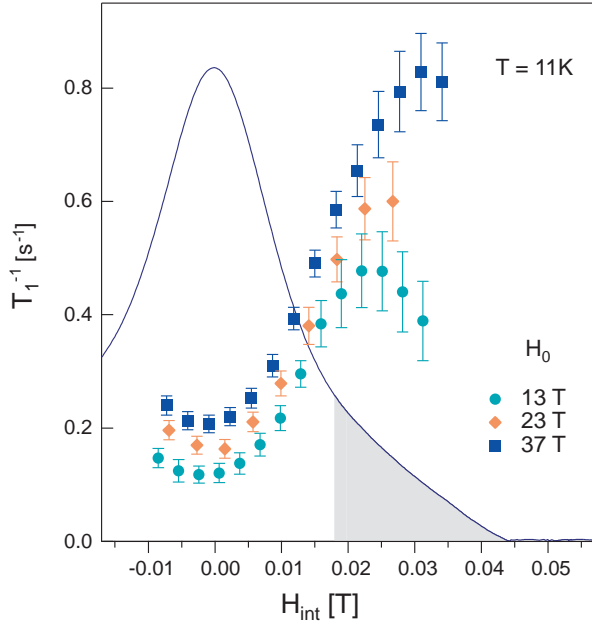


FIG. 2. Planar  $^{17}\text{O}$  spin-lattice relaxation rate across the vortex lattice NMR spectrum at 11 K. The spectrum is the  $-1/2 \leftrightarrow -3/2$  transition at 37 T. The shaded region is the estimated area occupied by the vortex cores at 37 T. We used a superconducting magnet, 13 T; a Bitter-style electromagnet, 23 T; and a hybrid of the two technologies, 37 T. We obtained precise spectra using a field sweep technique and we measured the relaxation rate using progressive saturation [10].

field up to 37 T, we sweep through a significant range of corresponding Zeeman energies,  $\sim \pm 2.5$  meV, larger than the thermal energy.

Our aligned powder sample of  $\text{YBa}_2\text{Cu}_3\text{O}_{7-\delta}$  is near-optimally doped and  $\sim 60\%$   $^{17}\text{O}$ -enriched. The crystal  $\hat{c}$ -axis was aligned with the direction of the applied magnetic field. Low-field magnetization data show a sharp transition at  $T_c(0) = 92.5$  K. High magnetic fields are essential to increase sensitivity to vortex cores by increasing their fraction of the NMR spectrum. In a field of 37 T vortices are  $\sim 80$  Å apart as compared with their core radius given by the size of the electron-pair wavefunction,  $\xi \approx 16$  Å, and so the cores occupy  $\sim 15\%$  of both the total volume of the sample and the NMR spectrum. We have shaded the corresponding region in Fig. 2. The high field also suppresses spin diffusion and vortex vibrations which complicate interpretation of the spin lattice relaxation at low field [7].

For high-temperature superconductors the gap in the excitation spectrum,  $\Delta_{\mathbf{k}}$ , is believed to have  $d$ -wave symmetry, implying that there are 4 nodes on the Fermi surface where the gap vanishes. At low temperature the electronic excitations, called quasiparticles, come exclu-

sively from the nodal regions shown in Fig. 3. They can be probed with NMR spin lattice relaxation, with the rate given by,

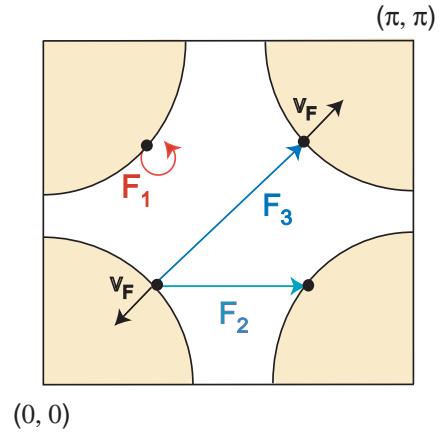


FIG. 3. Sketch of the Fermi surface for YBCO and the three processes that contribute to the NMR rate at low temperatures. The three processes,  $F_1$ ,  $F_2$ , and  $F_3$ , correspond to the choice of nodes, points where superconductivity is fully suppressed, (black dots) for the initial and final quasiparticle states. The spin lattice relaxation rate is given by,  $T_1^{-1} \sim \langle N_i(\epsilon)N_f(\epsilon) \rangle$ , where  $N_\alpha = \sum_{\mathbf{k}} \delta(\epsilon - E_{\mathbf{k},\alpha})$  are the initial ( $\alpha = i$ ) and final ( $\alpha = f$ ) density of states (DOS) respectively. The sum over wavevector  $\mathbf{k}$  is restricted to the regions around the nodes,  $\mathbf{k}_\alpha$ , and the product of the DOS is integrated over energy  $\epsilon$  in the range  $k_B T$  near the Fermi energy,  $E_F$ . The excitation energies  $E_{\mathbf{k},\alpha}$  for quasiparticles moving in the superflow field with momentum  $\mathbf{p}_s$  are Doppler shifted by an amount  $D_\alpha = \mathbf{v}_{F,\alpha} \cdot \mathbf{p}_s$ , where the Fermi velocity at node  $\mathbf{k}_\alpha$  is given in terms of the normal state excitation energy  $\epsilon_{\mathbf{k}}$  by,  $\mathbf{v}_{F,\alpha} = \partial \epsilon_{\mathbf{k}} / \partial \mathbf{k}|_{\mathbf{k}=\mathbf{k}_\alpha}$ . Note that for process  $F_3$  the relation  $D_i = -D_f$  holds, in contrast to, for example, process  $F_1$  where  $D_i = D_f$ . In sufficiently high magnetic field the Zeeman energy, becomes important and enters initial and final states with different signs ( $Z_{i,f} = \pm Z$ ), leading to,  $E_{\mathbf{k},\alpha} = \sqrt{\epsilon_{\mathbf{k}}^2 + \Delta_{\mathbf{k}}^2} - Z_\alpha + D_\alpha$ . Since the DOS depends linearly on energy near the nodes, the NMR rate is proportional to the product given by Eq. 1.

$$T_1^{-1} \sim \langle |\epsilon - Z + D_i| |\epsilon + Z + D_f| \rangle, \quad (1)$$

where  $\epsilon$  is of the order of  $k_B T$ ;  $Z = -\frac{1}{2}\gamma_e \hbar H_0$ , is the Zeeman energy;  $D_\alpha = \mathbf{v}_{F,\alpha} \cdot \mathbf{p}_s$  is the Doppler shift, and  $\alpha = i, f$  corresponds to initial and final electronic states near the nodes. Depending on the relative magnitude of  $k_B T$ ,  $Z$ , and  $D$  the dependence of the relaxation rate on temperature and field will show different behavior for each of three processes shown in Fig. 3. We can vary the first two terms,  $k_B T$ ,  $Z$ , by changing temperature and magnetic field. The Doppler term is proportional to the vortex currents, and varies with internal field,  $H_{int}$ , across the NMR spectrum. This term is a microscopic analogue of the classical frequency shift of a wave in a

moving reference frame, the latter being associated with the superconducting condensate.

At the peak of the NMR spectrum,  $H_{int} = 0$  in Fig. 2, we observe that the rate increases as a function of the external field,  $H_0$ . This dependence comes from the Zeeman interaction. The Doppler term is small in this region since the supercurrents cancel at the saddle-point. As we increase the applied field the Zeeman interaction dominates the energy spectrum near the nodes, i.e.  $Z$ , equivalent to 25 K at 37 T, is larger than  $k_B T$  at 11 K, and from Eq. 1 the NMR rate rises quadratically with field as  $\langle |Z^2 - \epsilon^2| \rangle$ .

To the right of the peak in the spectrum toward the vortex core, Fig. 2, we find that the rate increases by a factor of  $\sim 4-5$ . Here the superflow momentum increases sufficiently that the Doppler term in Eq. 1 becomes large compared to both  $Z$  and  $k_B T$  and it dominates the quasi-particle energy. Our observations show that  $T_1^{-1}$ , and consequently the density of electronic states (DOS), depends on distance,  $r$ , from the core. In particular, we expect the rate to increase as  $T_1^{-1} \sim (p_s)^2 \sim r^{-2}$ . The enhancement of  $T_1^{-1}$  depends only on  $r$  and should not be dependent on the applied magnetic field other than the Zeeman interaction. This is not to be confused with Volovik's prediction [11] that the average DOS,  $\langle N(0) \rangle \sim \sqrt{H_0}$ , which corresponds to  $\langle T_1^{-1} \rangle \sim H_0 \ln H_0$  where the average is over the entire spectrum. For conventional superconductors without nodes, the Doppler term has a negligible effect. Our observation of the Doppler shift extending to the saddle-point region shows that, even in high magnetic fields, the superconducting gap has well defined nodes.

Outside the vortex core we find that the effect of applied magnetic field from 13 to 37 T is simply to displace the relaxation rate data on a vertical scale in Fig. 2. This is possible if the Doppler term in Eq. 1 changes sign for initial and final states, just like the Zeeman term, and can only occur if those quasiparticle states are not from the same node. Then, at low temperatures, the rate is  $\sim D^2 + Z^2$  and increases quadratically with field. Otherwise, initial and final states come from the same node and the rate is  $\sim D^2 - Z^2$ , having the wrong field dependence in the regime  $D > Z$ . We have calculated the relative strengths of the three possible processes and their dependence on magnetic field. The calculation is performed using the known geometric form factors and the imaginary part of the electronic susceptibility which we extract by fitting the data. To account for our observed field dependence, the spin susceptibility must be strongly peaked near a wavevector corresponding to the  $F_2$  or  $F_3$  process, at least a factor of 7 greater than that at zero wavevector. This indicates that strong antiferromagnetic correlations between quasiparticles coexist with superconductivity at low temperatures. Antiferromagnetically correlated quasiparticles were identified by neutron scattering [1] in LSCO, a related compound, and are now confirmed in YBCO from NMR. Lake *et al.* speculated that if there was antiferromagnetism in the vortex core it

might polarize the intervening medium and account for their experiment.

Near the vortex core, the NMR rate decreases after reaching a maximum in the applied field of 13 T as shown

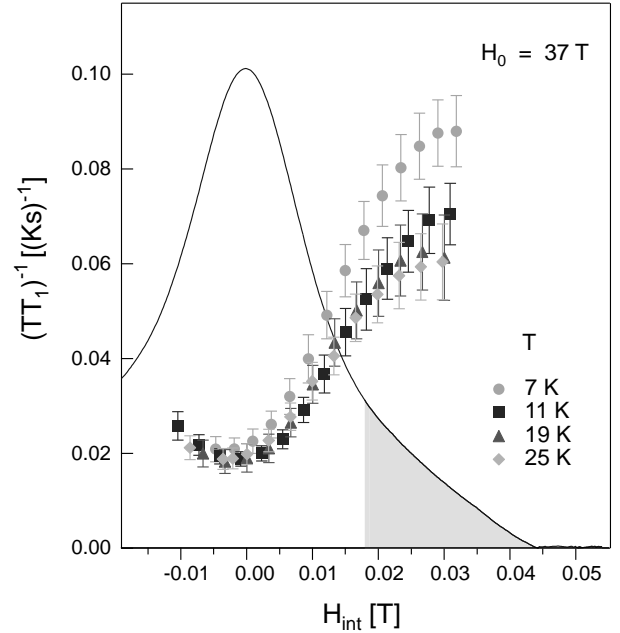


FIG. 4. Spin-lattice relaxation rate of planar  $^{17}\text{O}$  divided by temperature as a function of internal magnetic field. The shaded region is the area occupied by the vortex cores at 37 T. For a  $d$ -wave superconductor in the temperature range where  $k_B T$  is much less than  $\gamma_e \hbar H_0$ ,  $(T_1 T)^{-1}$  is expected to be constant. We clearly observe this behavior near the peak in the NMR spectrum.

in Fig. 2, reflecting a drop-off in  $p_s$ . At higher applied fields the rate increases significantly, well beyond its maximum value at 13 T. This increase with field exceeds that measured outside the cores by a factor of four and is most pronounced at the lowest temperatures, Fig. 4. We attribute this substantial excess rate to vortex core states. When superconductivity is suppressed near surfaces or in the vortex core, localized electronic states, called Andreev bound states, can appear [9,12]. Their signature is a peak in the density of states at the Fermi energy, called a zero-bias anomaly in tunneling experiments. Similar behavior might be expected in the vortex core of a high temperature superconductor. If we interpret our relaxation rate in the same way as for quasiparticles outside the cores, following the discussion in the caption to Fig. 3 and Eq. 1, then both field and temperature dependence are opposite to what is required for the zero-bias anomaly. Consequently, instead of a peak in the density of states there is a mini-gap,  $\sim \pm 5$  meV, much sharper than the variation of the DOS outside the vortex core. Previous reports of vortex core states have been based on charge tunneling in YBCO [13] and BSSCO [14]. Near  $E_F$ ,  $\sim \pm 5.5$  meV for YBCO, an added structure in the

DOS from the vortex core region separated by a mini-gap was observed. This surprising result is inconsistent with theoretical predictions [15]. Furthermore, tunneling is extremely sensitive to the surface and depends on an understanding of the tunneling matrix elements [16]. In contrast NMR probes bulk material. And yet, both experiments can have a similar interpretation.

NMR is directly sensitive to the magnetic character of electronic excitations. So an alternate explanation of our results for the vortex core region might involve antiferromagnetism as predicted [2] from a  $SO(5)$  nonlinear  $\sigma$  model. In this case field induced antiferromagnetic excitations could strongly enhance the NMR rate consistent with our observations. In future work, spatially resolved NMR relaxation experiments can be extended to understand the effects of doping on vortex core states and possibly identify a connection with the spin-pseudogap found in the normal state.

- 
- [1] Lake, B. *et al.* Spins in the Vortices of a High-Temperature Superconductor. *Science* **291**, 1759 (2001).
  - [2] Arovas D.P., Berlinsky A.J., Kallin C. & Zhang, S.C. Superconducting Vortex with Antiferromagnetic Core. *Phys. Rev. Lett.* **79**, 2871 (1997).
  - [3] Takigawa M., Ichioka M. & Machida K. Theory of vortex excitation imaging via an NMR relaxation measurement. *Phys. Rev. Lett.* **83**, 3057 (1999).
  - [4] Wortis R., Berlinsky A. J. & Kallin C. Spin-lattice relaxation in the mixed state of  $YBa_2Cu_3O_{7-\delta}$  and Doppler-shifted  $d$ -wave quasiparticles. *Phys. Rev. B* **61**, 12342 (2000).
  - [5] Morr D. K. & Wortis R. Theory of NMR as a local probe for the electronic structure in the mixed state of the high- $T_c$  cuprates. *Phys. Rev. B* **61**, R882 (2000).
  - [6] Reyes A. P. *et al.* Vortex melting in polycrystalline  $YBa_2Cu_3O_{7-\delta}$  from  $^{17}O$  NMR. *Phys. Rev. B* **55**, R14737 (1997).
  - [7] Curro N. J., Milling C., Haase J. & Slichter C. P. Local-field dependence of the  $^{17}O$  spin-lattice relaxation and echo decay rates in the mixed state of  $YBa_2Cu_3O_7$ . *Phys. Rev. B* **62**, 3473 (2000).
  - [8] Brandt E. H. Precision Ginzburg-Landau solution of ideal vortex lattice for any induction and symmetry. *Phys. Rev. Lett.* **78**, 2208 (1997).
  - [9] Hess H.F., Robinson R.B., Dynes R.C., Valles J.M. & Waszczak J.V. Vortex-core structure observed with a Scanning-tunneling-microscope observations of the Abrikosov flux lattice and the density of states near and inside a fluxoid. *Phys. Rev. Lett.* **62**, 214 (1989).
  - [10] Mitrović V. F., Sigmund E. E. & Halperin W. P. Progressive Saturation NMR Relaxation, *Phys. Rev. B* **64**, 024520 (2001).
  - [11] Volovik G. E. Superconductivity with lines of Gap nodes: density of states in the vortex. *JETP Lett.* **58**, 469 (1993).
  - [12] Lesueur J., Greene L. H., Feldmann W. L., & Inam A., Zero bias anomalies in  $YBa_2Cu_3O_7$  tunnel-junctions. *Physica (Amsterdam)* **191C**, 325 (1992).
  - [13] Maggio-Aprile I., Renner Ch., Erb A., Walker E. & Fischer Ø. Direct Vortex Lattice imaging and Tunneling spectroscopy of Flux Lines on  $YBa_2Cu_3O_{7-\delta}$ . *Phys. Rev. Lett.* **75**, 2754 (1995).
  - [14] Pan S. H. *et al.* STM Studies of the Electronic Structure of Vortex Cores in  $Bi_2Sr_2CaCu_2O_{8+\delta}$ . *Phys. Rev. Lett.* **85**, 1536 (2000).
  - [15] Franz M. & Tešanović Z. Self-consistent electronic structure of a  $d_{x^2-y^2}$  and a  $d_{x^2-y^2} + id_{xy}$  vortex. *Phys. Rev. Lett.* **80**, 4763 (1998).
  - [16] Wu C., Xiang T., Su Z. Absence of the zero bias peak in vortex tunneling spectra of high-temperature superconductors. *Phys. Rev. B* **62**, 14427 (2000).

## Acknowledgements

This work was supported by the Science and Technology Center for Superconductivity, the Materials Research Center at Northwestern University, and the National High Magnetic Field Laboratory supported by the National Science Foundation and the State of Florida. ME acknowledges support from U.S. Dept. of Energy, Office of Science. We are grateful to J. A. Sauls, J. Moreno, R. Wortis and K. Machida for helpful discussions.

Correspondence and requests for materials should be addressed to W.P.H. (e-mail: w-halperin@northwestern.edu).